Doping-dependent study of the periodic Anderson model in three dimensions

Thereza Paiva*
Instituto de Física, Universidade Federal do Rio de Janeiro, Caixa Postal 68.528, 21945-970 Rio de Janeiro, Brazil

Gökhan Esirgen† and Richard T. Scalettar
Department of Physics, University of California, Davis, California 95616-8677, USA

Carey Huscroft
Hewlett-Packard Company, Roseville, California 95747-5200, USA

A. K. McMahan
Lawrence Livermore National Laboratory, University of California, Livermore, California 94550-9234, USA
(Received 19 August 2003; published 17 November 2003)

We study a simple model for *f*-electron systems, the three-dimensional periodic Anderson model, in which localized *f* states hybridize with neighboring *d* states. The *f* states have a strong on-site repulsion which suppresses the double occupancy and can lead to the formation of a Mott-Hubbard insulator. When the hybridization between the *f* and *d* states increases, the effects of these strong electron correlations gradually diminish, giving rise to interesting phenomena on the way. We use the exact quantum Monte Carlo, approximate diagrammatic fluctuation-exchange approximation, and mean-field Hartee-Fock methods to calculate the local moment, entropy, antiferromagnetic structure factor, singlet correlator, and internal energy as a function of the *f*-*d* hybridization for various dopings. Finally, we discuss the relevance of this work to the volume-collapse phenomenon experimentally observed in *f*-electron systems.

DOI: 10.1103/PhysRevB.68.195111 PACS number(s): 71.10.Fd, 71.27.+a, 71.15.Nc, 64.70.Kb

I. INTRODUCTION

The periodic Anderson model (PAM) describes the qualitative physics of solids in which a set of localized (*f*) orbitals having a strong on-site repulsion hybridizes with another set of noninteracting conduction (*d*) orbitals.[1] The basic magnetic features encapsulated in the PAM include the formation of moments on the localized orbitals due to the suppression of double occupancy by the repulsion. The magnetic nature of the ground state is determined by the strength of the hybridization between the localized and conduction electrons.[2] If the hybridization is small, then the magnetic ordering of the localized moments takes place through the establishment of a modulation of the conduction-electron spin density, an indirect Ruderman-Kittel-Kasuya-Yosida coupling.[3] For strong hybridization the screening of magnetic moments of the correlated electrons by conduction electrons (Kondo screening) is expected. While some of these general ideas are well accepted, others are still under study.[4] For example, Noziere's notion of ''exhaustion,''[5] that only the conduction electrons near the Fermi surface can participate in singlet formation and hence there are not enough of them to form singlets with all the local spins, has received considerable recent scrutiny.[6] Related to this is the effectiveness of the compensating cloud around each localized orbital. The size of this cloud has been a subject of controversy. Arguments based on scaling and renormalization-group ideas for the single-impurity Kondo point to a cloud with length $\xi_K \sim v_F/T_K$, where v_F is the Fermi velocity and T_K is the Kondo temperature.[7,8] Since Kondo temperatures are normally of the order of tens of degrees, this leads to a large Kondo cloud of the order of thousands of lattice spacings *a*. On the other hand, similar arguments for the single-impurity multichannel Kondo model have led Gan[9] to find $\xi_K \sim a$. This cloud has never been observed experimentally and Knight shift experiments from Boyce and Slichter[10] were interpreted to indicate the absence of a large cloud.

The charge excitations of the PAM also show interesting features. As in the one-band Hubbard model, a strong repulsion on the localized orbitals makes them exhibit the characteristics of a Mott insulator, including a suppression of the *f* density of states and a vanishing *f*-electron compressibility.[11] The density of states can also exhibit a Kondo resonance as it evolves to a single broad peak at weak coupling.[11]

While many of these general ideas are well accepted, much of the quantitative physics of the PAM remains open. Only relatively recently has the phase diagram of the PAM been studied by non-mean-field approaches such as the determinant quantum Monte Carlo[12,13] (QMC) and dynamical mean-field theory[14] (DMFT). The former provides an exact treatment of correlations on finite lattices but is computationally demanding and therefore has so far been restricted in its applications to the particle-hole symmetric point, where both *f* and *d* orbitals are half filled. The DMFT approach works explicitly in the thermodynamic limit and hence can observe finite-temperature phase transitions without recourse to finite-size-scaling techniques, but it involves the approximation of ignoring the momentum dependence of the self-energy.

There are several reasons to believe that the removal of the restriction of half filling might reveal different physics. First, half filling is the most optimal electron density for antiferromagnetism. Since a number of the potential systems for which the PAM has been suggested as an appropriate

Hamiltonian do not exhibit such magnetic correlations, it is desirable to study the properties of the doped system, for which antiferromagnetism is considerably suppressed.

Second, the noninteracting bands have special features which are unique to half filling. For example, in the absence of interactions, the canonical choice of a momentum-independent hybridization $V_{\mathbf{k}}=V$, which corresponds to a hybridization of the localized orbitals with the conduction orbitals on the same site, gives rise to a band insulator at half filling. Meanwhile, the choice $V_{\mathbf{k}}=-2V(\cos k_x+\cos k_y+\cos k_z)$, which, instead, hybridizes the localized orbitals with the conduction orbitals on the nearest-neighbor sites,[15] leads to a metallic state at half filling; yet, this hybridization $V_{\mathbf{k}}$ vanishes at the half-filled Fermi surface and, therefore, is also somewhat artificial. While the addition of strong correlations is expected to modify the physics greatly, it is still possible that the properties of the PAM reflect these special features of the noninteracting limit at half filling.

Finally, the particle-hole symmetric point is a very special one for analytic theories. For example, second-order perturbation theory (SOPT) in the on-site interaction becomes exact at the *strong-coupling* limit, in addition to being exact at the weak-coupling limit. This odd result is only true at half filling and, indeed, is only true for models with a single-impurity band hybridizing with a single conduction band. Studying the PAM off half filling will therefore give valuable insight into the nature of analytic approaches to the case of multiband systems, where this anomalous success of SOPT does not occur at any filling.

A specific instance where all three issues come into play is the Anderson impurity model and the PAM as they are applied to the cerium (Ce) volume collapse.[16–19] While recent QMC studies of the half-filled PAM have lent greater quantitative understanding of this problem,[20] the relevance of this work for the Ce volume-collapse phenomenon would be much better justified if the same physics could be demonstrated in the doped system.

In this paper we will present a detailed study of the magnetic, charge, and thermodynamic properties of the PAM for various band fillings. We will make use of the exact QMC, approximate diagrammatic fluctuation-exchange approximation (FLEX), and mean-field Hartree-Fock (HF) methods. We will concentrate on the effects of doping of additional electrons into the system for parameter regimes where the number of localized (i.e., f) electrons still remains approximately 1. This is a natural consequence of the Mott-Hubbard gap in the PAM and similarly is also the experimental situation in at least one application of interest—the Ce volume-collapse transition.

Our key conclusions are the following. (1) The more accurate treatment of correlations provided by QMC and FLEX shift the HF transition to stronger coupling and decrease its sharpness. HF for the PAM gives more accurate energies at low temperatures near strong coupling than weak. (2) Antiferromagnetic correlations remain robust for a range of dopings of the conduction band. By comparison the one-band Hubbard model loses its long-range antiferromagnetic order more rapidly upon doping.[21–23] (3) Anomalies in the singlet correlator, entropy, and internal energy persist even when the f-d hybridization has substantial values on the Fermi surface. They also persist to doping levels where antiferromagnetic correlations have been eliminated. However, their sharpness does appear correlated with the presence of magnetism. (4) FLEX captures many of the same qualitative features exhibited by QMC in the dependence on the interband hybridization of the local moment, antiferromagnetic correlations, entropy, and internal energy, especially at weak coupling, where the HF internal energy is not very accurate. At the same time, as is well known, FLEX has difficulty reproducing the Mott-Hubbard gap in the strong-coupling limit.[24]

II. MODEL AND METHODS

A. Periodic Anderson model

We will study the grand-canonical Hamiltonian

$$\mathcal{H}-\mu\mathcal{N}=\sum_{\langle \mathbf{i},\,\mathbf{j}\rangle,\;\sigma}\{[-t_{dd}d^{\dagger}_{\mathbf{i}\sigma}d_{\mathbf{j}\sigma}-t_{fd}(d^{\dagger}_{\mathbf{i}\sigma}f_{\mathbf{j}\sigma}+f^{\dagger}_{\mathbf{i}\sigma}d_{\mathbf{j}\sigma})] + \mathrm{H.c.}\}+\varepsilon_f\sum_{\mathbf{i},\;\sigma}n_{f\mathbf{i}\sigma}-\mu\sum_{\mathbf{i},\;\sigma}(n_{d\mathbf{i}\sigma}+n_{f\mathbf{i}\sigma}) + U_f\sum_{\mathbf{i}}n_{f\mathbf{i}\uparrow}n_{f\mathbf{i}\downarrow}. \quad (1)$$

$d^{\dagger}_{\mathbf{i}\sigma}$ and $f^{\dagger}_{\mathbf{i}\sigma}$ create d (conduction) and f (localized) electrons with spin σ on the lattice site $\mathbf{i}$. We consider a three-dimensional periodic simple-cubic lattice, where $\langle \mathbf{i},\,\mathbf{j}\rangle$ is a sum over nearest-neighbor bonds. Therefore, this term represents the nearest-neighbor hybridization integrals (i.e., hoppings) of the d-d (t_{dd}) and d-f (t_{fd}) orbitals. The remaining one-particle terms are ε_f, which measure the f-orbital energy level with respect to that of the d orbital (which was chosen to be zero by convention), and the chemical potential μ. The charge-density operator on site $\mathbf{i}$ in orbital d with spin σ is $n_{d\mathbf{i}\sigma}=d^{\dagger}_{\mathbf{i}\sigma}d_{\mathbf{i}\sigma}$ and similarly for $n_{f\mathbf{i}\sigma}$. Finally, U_f describes an effective on-site repulsion between the localized f electrons.

When the hopping term is Fourier transformed, the resulting expression is $\Sigma_{\mathbf{k},\,\sigma}[\varepsilon_{\mathbf{k}}d^{\dagger}_{\mathbf{k}\sigma}d_{\mathbf{k}\sigma}+V_{\mathbf{k}}(d^{\dagger}_{\mathbf{k}\sigma}f_{\mathbf{k}\sigma}+f^{\dagger}_{\mathbf{k}\sigma}d_{\mathbf{k}\sigma})]$, with $\varepsilon_{\mathbf{k}}=-2t_{dd}(\cos k_x+\cos k_y+\cos k_z)$ and $V_{\mathbf{k}}=-2t_{fd}(\cos k_x+\cos k_y+\cos k_z)$. The particular choice of $\varepsilon_f=-U_f/2$ and $\mu=0$ results in $\langle n_d\rangle=\langle n_f\rangle=1$ ($\langle n_d\rangle\equiv\Sigma_{\sigma}\langle n_{d\mathbf{i}\sigma}\rangle$ etc.). This is the so-called "symmetric" PAM, in which both orbitals are half filled regardless of the choice of all the other parameters and temperature.

We will express all energy units in this paper in terms of $t_{dd}\equiv 1$. We will also set $U_f/t_{dd}=6$ throughout the paper and vary t_{fd}/t_{dd} for several fillings and ε_f/t_{dd}. For α- and γ-Ce, respectively, calculated values for the effective hopping and Coulomb-repulsion parameters in eV are $t_{dd}\approx 0.90$ and 0.74, $t_{fd}\approx 0.19$ and 0.14, $U_f\approx 5.7$ and 5.9.[18] Our choices of the model parameters are therefore in rough agreement with the values for cerium. Finer tuning would not be useful given the approximations inherent in using a two-band model.[25]

B. Determinant quantum Monte Carlo

The determinant-QMC method that we employ is standard and has been described many times in the literature.[26]

Its key features are an exact treatment of the interactions via a path-integral representation of the partition function and the decoupling of the interaction via the introduction of a Hubbard-Stratonovich field, whose possible configurations are then summed over stochastically. The approach is able to study several hundred interacting electrons, much greater than other exact approaches like diagonalization, but still representing small lattices, especially in three dimensions. This is an especially serious consideration in determining the presence or absence of long-range order. Local quantities such as the internal energy and near-neighbor spin correlations have much smaller finite-size effects. The simulations reported here are on lattices of 64 ($4\times4\times4$) spatial sites with fillings ranging from $\langle n\rangle=2.0$ to $\langle n\rangle=3.6$ electrons per site, where $\langle n\rangle\equiv\langle n_d\rangle+\langle n_f\rangle$.

Besides finite spatial-lattice size, a crucial bottleneck in the determinant QMC is the ''sign problem,''[27] which, roughly speaking for this application, restricts the temperatures accessible to simulation to those greater than $T\sim W/50$, where W is the noninteracting bandwidth.

C. Fluctuation-exchange approximation

We will also study the PAM using the FLEX approximation.[28] The FLEX approximation can be motivated in various different ways. It can be thought of as an extension of the Hartree-Fock theory, in which the bare interaction is self-consistently screened by the exchange of electron-hole and electron-electron (two-particle) fluctuations. Or it can be viewed as a conserving approximation within the framework of Baym-Kadanoff's generating-functional formalism.[29] Another view is as an extension of the random-phase approximation (RPA), in which the two-particle propagators of RPA are self-consistently included in the self-energy. Yet another, but a very elegant one, is that FLEX is the first step in the parquet-approximation's[30] two-particle self-consistency scheme.

FLEX suffers from lack of the two-particle self-consistency found in the parquet approximation, which renormalizes the bare vertices (which are used to calculate the fluctuation propagators) with vertex corrections. Although it is possible to formulate FLEX to work in spontaneously-broken-symmetry states (with an anomalous self-energy), such as a magnet or a superconductor, FLEX as commonly practiced rarely does so. The only such FLEX calculations to this date include those for a superconductor.[31] For previous results using FLEX for Hubbard-like models, along with comparisons with QMC, see Ref. 32.

The normal-state FLEX solutions of Hubbard-like models are also known to give the incorrect strong-coupling limit. It is not known if the broken-magnetic-symmetry solutions may give the right limit for main thermodynamic quantities at strong coupling.

The FLEX approximation used in this paper incorporates all four channels (density, magnetic, singlet, and triplet fluctuations). In order to satisfy certain symmetries, all these four channels are needed. In fact we also tested FLEX without using the particle-particle fluctuations, and it turned out that the resulting accuracy is lower. We also use the numerical renormalization-group method on the Matsubara frequencies to accelerate evaluation of the FLEX self-energies and fluctuation propagators.[33]

III. RESULTS AND DISCUSSION

In this section we will show how the properties of the PAM evolve from strong to weak coupling at several different fillings. We begin by describing the orbital occupations, showing how the charge is transferred with the temperature. This helps establish relevant temperature scales in these simulations. We then show short-range magnetic correlations—measures of the local moment and singlet formation—before turning to the issue of long-range antiferromagnetism. The section concludes with results for the entropy and internal energy and a general discussion of the relation of their behavior with magnetism.

As mentioned in Sec. II A, the PAM Hamiltonian in Eq. (1) with $\varepsilon_f=-U_f/2$ and $\mu=0$ has particle-hole symmetry—$\langle n_d\rangle=\langle n_f\rangle=1$—i.e., both conduction and localized orbitals are half filled, regardless of all other parameters. We will compare the properties of the PAM at two electron densities with the behavior at half filling. The density $\langle n\rangle=2.2$ is only lightly doped away from half filling and allows us to examine the rapidity of the destruction of the antiferromagnetism. The density $\langle n\rangle=2.6$, as we shall see, is large enough that all traces of long-range order have been suppressed. In both these cases, we have adjusted the f site energy to maintain $\langle n_f\rangle\sim1$.

Finally, we also present a few results for an extreme-filling case, in which $\langle n_d\rangle\sim1.8$ and $\langle n_f\rangle\sim1.8$, where the effect of electron-electron correlations are shown to be minimal, as is expected since this is equivalent to a very low electron density by a particle-hole transformation.

A. Orbital occupations

We begin by examining the evolution of the local orbital density with the temperature T in Fig. 1. At high T the orbitals are equally filled since energies like ε_f, which distinguish the orbitals from each other, are washed out by large thermal fluctuations. As T is lowered, the occupations shift. By $T\sim0.125$ ($\beta\equiv1/T\sim8$), much, but not all, of the charge transfer from f to d orbitals is complete for this value of $t_{fd}=0.8$. For smaller t_{fd} the occupations reach their asymptotic ground-state values at higher temperatures owing to the presence of a larger Mott gap. Figure 1 also shows the data for the Hartree-Fock solutions to the problem, demonstrating that these techniques are in qualitative agreement with the exact QMC calculations for the temperature dependence of the orbital densities, despite the fact that Hartree-Fock predicts magnetic order below $T\sim U_f/4$ ($=1.5$ for $U_f=6$), well above any possible QMC transition temperature. The FLEX results are in even better qualitative agreement with the exact QMC results in the entire temperature range shown.

B. Local moment

Figure 2(a) shows the dependence of the f-orbital moment $\langle m_{ff}^2\rangle\equiv\langle(n_{f\mathbf{i}\uparrow}-n_{f\mathbf{i}\downarrow})^2\rangle=\langle n_f\rangle-2\langle n_{f\mathbf{i}\uparrow}n_{f\mathbf{i}\downarrow}\rangle$ on the hybridiza-

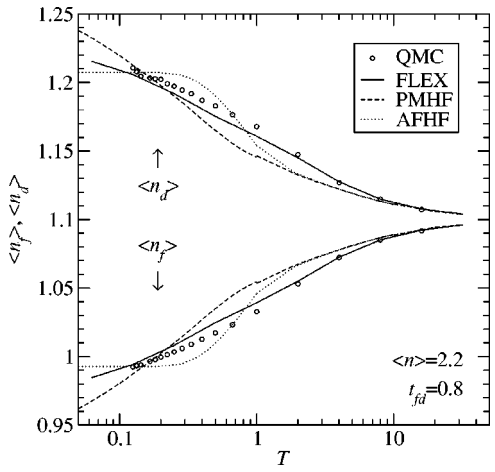

FIG. 1. The dependence of the *f* and *d* orbital occupations on the temperature T at $t_{fd}=0.8$ for $\langle n\rangle=2.2$. Other parameters are $t_{dd}=1$ and $U_f=6$ (throughout this paper), and $\varepsilon_f=-2.785$. Also, the lattice sizes in this paper are all $4\times4\times4$ unless otherwise specified. Results for QMC, FLEX, paramagnetic Hartree-Fock (PMHF), and antiferromagnetic Hartree-Fock (AFHF) are shown.

tion t_{fd} at low temperature. Here data for several dopings are shown. For all three cases, $\langle m_{ff}^2\rangle$ is fully formed at weak hybridization, and, as expected, it is reduced as t_{fd} increases and the system becomes less strongly correlated. Even for relatively large t_{fd}, however, $\langle m_{ff}^2\rangle$ is significantly enhanced over its uncorrelated value of $\langle m_{ff}^2\rangle=1/2$. For example, the value $\langle m_{ff}^2\rangle=0.8$ at $t_{fd}=1$ and $\langle n\rangle=2.2$ corresponds to a double occupation of $\langle n_{f\mathbf{i}\uparrow}n_{f\mathbf{i}\downarrow}\rangle=0.10$, a value reduced by a factor of 2.5 from the result in the absence of correlations, $\langle n_{f\mathbf{i}\uparrow}n_{f\mathbf{i}\downarrow}\rangle=\langle n_{f\mathbf{i}\uparrow}\rangle\langle n_{f\mathbf{i}\downarrow}\rangle=1/4$. Although the moment is reduced as t_{fd} increases, even at large t_{fd}, the moment is well enough formed to allow for interesting magnetic ordering to occur. For $U/t=4$, the half-filled one-band Hubbard model has $\langle m^2\rangle=0.77$ at low T, a value comparable to the smaller of those in Fig. 2(a); yet, the one-band Hubbard model still exhibits clear long-range antiferromagnetic order for this U/t. Later in this paper, we will examine antiferromagnetism in the PAM.

In Fig. 2(b) the FLEX results for the local and instantaneous component of the magnetic susceptibility, $\chi_m(\Delta\mathbf{R}=\mathbf{0},\Delta\tau=0)$, are shown for different lattice sizes.[34] This quantity is the equivalent of the local moment. As depicted in the figure, the FLEX and QMC results are very similar, although FLEX somewhat underestimates the local moment. The finite-size effects are very small, as would be expected for a local quantity.

C. Singlet correlator

We will now turn to the issue of the Kondo screening of the local moments. Here we probe the formation of local Kondo singlets, in which one conduction electron and one localized electron in nearest-neighbor sites form a bound singlet state. In order to do that we use the singlet correlator, which is the nearest-neighbor interband spin-spin correlation function and is defined by $c_{fd}=\frac{1}{3}\Sigma_{\mathbf{j}}^{nn}\langle\vec{S}_{f\mathbf{i}}\cdot\vec{S}_{d\mathbf{j}}\rangle$, where

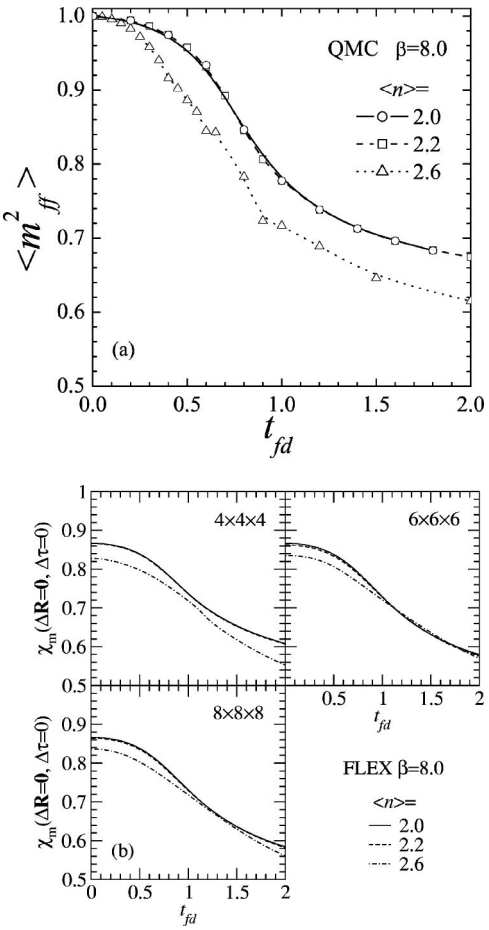

FIG. 2. (a) The dependence of the QMC local moment on the hybridization t_{fd} at low temperature $T=1/8$ ($\beta=1/T=8$) for $\langle n\rangle=2.0$, 2.2, and 2.6. $\varepsilon_f=-3.0$, -2.785, and -2.6, respectively. Other parameters are the same as in Fig. 1. (b) The FLEX results for the same parameters for three-different lattice sizes, showing finite-size effects are small. The quantity shown is the $\Delta\mathbf{R}=\mathbf{0}$, $\Delta\tau=0$ component of the *f*-orbital magnetic susceptibility, which is the same as the QMC local moment shown in (a) (Ref. 34). The QMC and FLEX results are very similar.

$$\vec{S}_{f\mathbf{i}}=(f_{\mathbf{i}\uparrow}^{\dagger}\ f_{\mathbf{i}\downarrow}^{\dagger})\vec{\sigma}\begin{pmatrix}f_{\mathbf{i}\uparrow}\\ f_{\mathbf{i}\downarrow}\end{pmatrix}$$

and likewise for $\vec{S}_{d\mathbf{j}}$. This definition of c_{fd} is a natural extension of the dot product of the local electron-spin and conduction electron spin on the same lattice site which is widely used to measure singlet formation within a PAM with on-site fd hybridization. As discussed above, our model has an intersite fd hybridization which leads to singlet formation of the local electron spin with conduction electrons on neighboring sites.[20]

In Fig. 3 we show the dependence of c_{fd} on the hybridization t_{fd} for different fillings, calculated by QMC. There is a qualitative difference between the $\langle n\rangle=2.6$ case, and the $\langle n\rangle=2.0$ and 2.2 cases. In the latter there is a sharp onset in the singlet correlator c_{fd} near $t_{fd}=0.6$. This was suggested to be intimately related to the Kondo volume-collapse scenario in our previous work for $\langle n\rangle=2.0$.[20] This onset moves

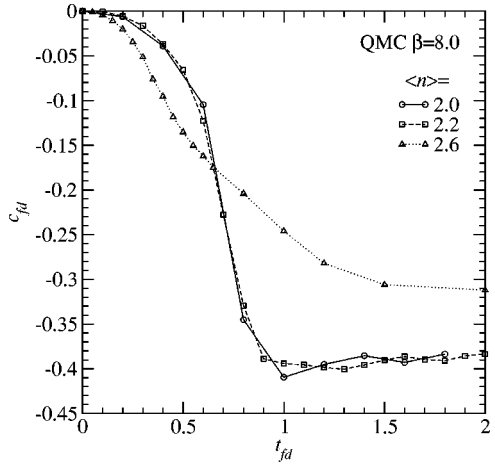

FIG. 3. The hybridization dependence of the singlet correlator, which measures the degree of the local antiferromagnetism between an f moment and the conduction-electron spins on the neighboring sites. Parameters are the same as in Fig. 2(a).

to smaller t_{fd} and becomes much less sharp at $\langle n\rangle = 2.6$. The $\langle n\rangle = 2.0$ and 2.2 cases are almost identical, as will be seen throughout this paper. Thus the fact that our choice of hybridization vanishes at the $\langle n\rangle = 2.0$ Fermi surface as noted earlier—but not at the $\langle n\rangle = 2.2$ Fermi surface—shows that the former artificiality has no impact on the conclusions in Ref. 20.

Let us call T_K the temperature where the local singlets are formed. We expect $T_K(t_{fd})$ to increase with t_{fd}.[2] The behavior of the singlet correlator in Fig. 3 can then be explained: the temperature used in the simulations ($T = 1/8$) crosses T_K. As the crossing point depends on band filling we observe different onsets, as discussed above. The crossing of T and T_K also explains why $c_{fd} \to 0$ for small t_{fd}.

D. Antiferromagnetism

Another possible phenomenon for the PAM is antiferromagnetic ordering of the moments. Figure 4(a) shows QMC results for the equal-time antiferromagnetic structure factor S_{ff}, the sum of the staggered correlations of the local f spins across the lattice, $S_{ff}(T, \mathbf{q}=(\pi,\pi,\pi)) = (2/3N)\Sigma_{\mathbf{i},\mathbf{j}}(-1)^{\mathbf{i}+\mathbf{j}}\vec{S}_{f\mathbf{i}}\cdot\vec{S}_{f\mathbf{j}}$. This structure factor is normalized in such a way that if there is only short-range magnetic order, S_{ff} is of order unity, whereas if there are long-range correlations S_{ff} is of order the lattice size (and hence diverges in the thermodynamic limit).

In Fig. 4(b) we show FLEX results for the instantaneous antiferromagnetic susceptibility χ_m. Just as the instantaneous, local susceptibility is the FLEX equivalent of the local moment, χ_m is the FLEX analog of the QMC structure factor.[34] We will discuss the issue of long-range order below. However before doing so, we emphasize the key observation that such an order for $\langle n\rangle = 2.6$ is clearly completely suppressed.

In interpreting these results further, and in particular the possible occurrence of long-range order at $\langle n\rangle = 2.0$ and $\langle n\rangle = 2.2$, it is important to emphasize that the Neél temperature depends on t_{fd}. As in the three-dimensional single-band Hubbard model, T_N is low at small t_{fd}, rises to a maximum, and then falls again at large t_{fd}. The important point is that a set of simulations at fixed temperature, such as those of Fig. 4, can potentially cut across the T_N vs t_{fd} curve, yielding the impression of the existence of AF order only in some intermediate range of t_{fd}. With this in mind, we believe the falloff of AF order at small t_{fd} for $\langle n\rangle = 2.0$ and 2.2 reflects only that T_N has gone below the simulation temperature. Meanwhile, the falloff at large t_{fd} may also reflect this reduction of T_N or the competing formation of Kondo singlets. We note that in the PAM with on-site hybridization, one expects singlet formation to usurp long-range magnetic order completely at large t_{fd}.[12] Our FLEX results suggest the in-

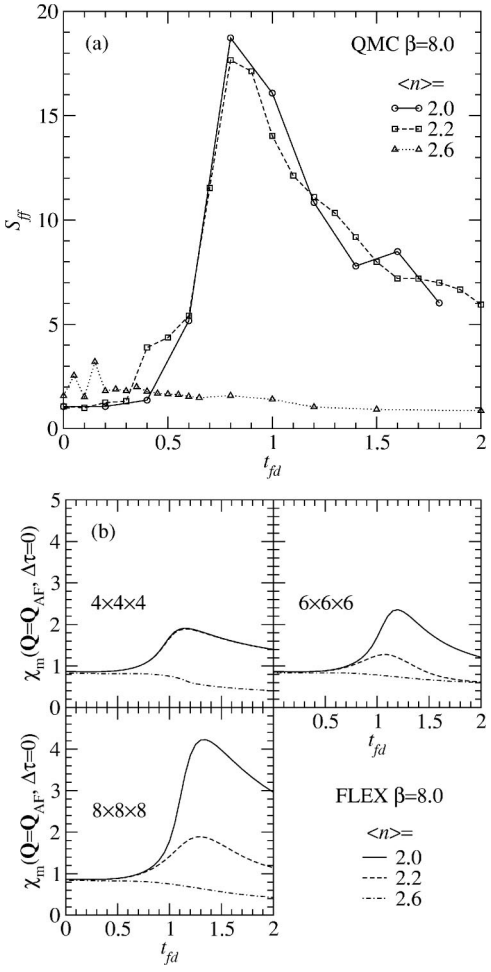

FIG. 4. (a) The dependence of the antiferromagnetic structure factor on the hybridization t_{fd}, as computed with QMC. Parameters are the same as in Fig. 2(a). (b) The FLEX results for the same parameters for three-different lattice sizes. The quantity shown is the $\mathbf{Q}=\mathbf{Q}_{\mathrm{AF}}=(\pi,\pi,\pi)$, $\Delta\tau=0$ component of the f-orbital magnetic susceptibility, which is the same quantity as in (a) [Ref. 34]. The QMC and FLEX results are very similar. Note the finite-size scaling of the FLEX results. That antiferromagnetism persists at large t_{fd}, when singlet formation is expected in the case of on-site hopping between f and d orbitals, reflects our near-neighbor choice of f-d hybridization. Antiferromagnetism is clearly absent for all t_{fd} at $\langle n\rangle = 2.6$.

tersite hybridization is different in this regard. Only a very detailed study including finite-size scaling can sort out these different possibilities.

To reemphasize, despite all these complications, Fig. 4 still carries an unambiguous message; the filling $\langle n\rangle = 2.6$ has a very different behavior in its magnetic properties: there is no long-range order. We have already seen that the singlet correlator still exhibits a growth with t_{fd} at $\langle n\rangle = 2.6$. Below we will see that, in the same way, the $\langle n\rangle = 2.6$ entropy and energy still behave rather similarly to cases where the densities are close to half filling.

E. Entropy

The low-temperature entropy $S(T = T_{\rm low})$ offers a means of probing Kondo-singlet formation as well as antiferromagnetic order. Specifically, the entropy per atom of free spin-$\frac{1}{2}$ moments is $\ln 2$, which can be reduced by the formation of local singlets in cooperation with the surrounding valence electrons or by the onset of magnetic order. Since the f and d subsystems decouple at small t_{fd}, the free-moment regime is realized by the f electrons in this strong-coupling limit for $T_{\rm low}$ above the Neél temperature $T_{\rm N}$, yet well below some characteristic temperature of moment formation. $T_{\rm low} = 0.125$ is a reasonable choice since Fig. 2(a) shows fully formed f moments at small t_{fd} for this temperature, while $T_{\rm N} \to 0$ as $t_{fd} \to 0$. The entropy of the d subsystem may be exactly calculated for $t_{fd} = 0$, and at $T_{\rm low} = 0.125$ has already reached its $T = 0$ limit: $S_d(t_{fd} = 0, T = 0) = 0.433\,22$, $0.294\,62$, and $0.312\,77$ for $\langle n\rangle = 2.0$, 2.2, and 2.6, respectively. These nonzero S_d values at $T = 0$ are finite-size effects of the $4 \times 4 \times 4$ lattice arising from the degeneracies of the d levels at the Fermi surface, which are a non-negligible fraction of states in the Brillouin zone for small lattices. The f electrons are moved away from the Fermi surface by the Mott-Hubbard gap and are not affected by such finite-size effects. We calculate the entropy for the fully interacting system from

$$S(t_{fd}, T) = S_\infty - \int_T^\infty dT' \frac{1}{T'} \frac{\partial E(t_{fd}, T')}{\partial T'} \tag{2}$$

and

$$S_\infty = 4 \ln 4 - \langle n\rangle \ln\langle n\rangle - (4 - \langle n\rangle)\ln(4 - \langle n\rangle), \tag{3}$$

using fits to the QMC energies as described elsewhere.[20,35]

In Fig. 5 we show the dependence of the low-T entropy on the hybridization t_{fd} at $T = 0.125$. In order to make the analysis of the entropy more meaningful, we plot $S(t_{fd}, T) - S_d(t_{fd} = 0, T = 0)$ as a function of t_{fd}. After this subtraction the entropy curves in Fig. 5 start with the value $\ln 2$ at $t_{fd} = 0$, reflecting the free f moments. The FLEX results are slightly off, representing the weak-coupling nature of the approximation, but it is very interesting to see such a weak-coupling diagrammatic approximation doing so well at the strong-coupling limit, capturing all of the local-moment entropy at the lower fillings and 90% at the highest filling. For $\langle n\rangle = 2.0$ the QMC entropy starts to drop around $t_{fd} = 0.6$; this value moves down to a smaller value of $t_{fd} = 0.2$ for

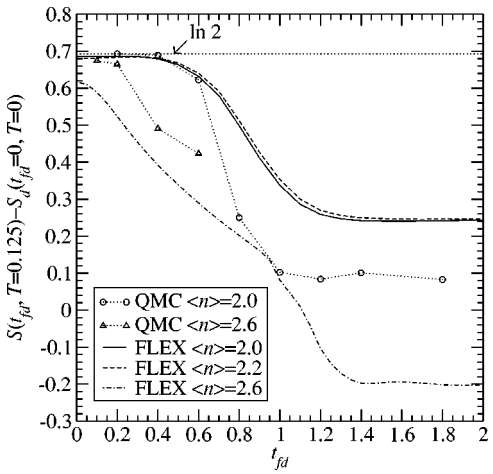

FIG. 5. The dependence of the entropy on the hybridization t_{fd}. Both QMC and FLEX results are shown. Parameters are the same as in Fig. 2(a), and the $t_{fd} = 0$ entropy of the d system is removed as discussed in the text. The QMC and FLEX results agree rather well, especially in the atomic ($t_{fd} = 0$) limit where they produce the $\ln 2$ entropy due to the formation of local moments.

$\langle n\rangle = 2.6$. One note should be added at this point; as the entropy drop for $\langle n\rangle = 2.6$ took place at a smaller t_{fd}, we did not pursue calculations for higher t_{fd} values. From Eq. 2 it is clear that a thin grid of temperatures is needed to get the entropy for a given t_{fd}. We were not able to reach the needed low temperatures due to "sign problems," as mentioned in Sec. II B. The drop in the entropy is also sharper in the $\langle n\rangle = 2.0$ case. The $\langle n\rangle = 2.2$ results (only shown for FLEX) are almost identical to the $\langle n\rangle = 2.0$, as seen in other quantities as already noted. The FLEX and QMC results still do not fully agree as one approaches $t_{fd} = 2$ (weaker coupling) because FLEX becomes truly valid only for $t_{fd} \gtrsim 3$, as we will show in the following section.

Examination of the singlet correlator (Fig. 3) and antiferromagnetic structure factor (Fig. 4) suggests that the sharp drop in the entropy for the $\langle n\rangle = 2.0$ and 2.2 cases could be related to both the formation of the Kondo singlets and the onset of the antiferromagnetism. Magnetic order, however, is ruled out for the $\langle n\rangle = 2.6$ case, where there is nevertheless still a significant drop in the entropy with increasing t_{fd}.

F. Internal energy

In this section we present results for the internal energy as a function of t_{fd} at the relatively low temperature of $T = 0.125$ (in one case 0.167). Because the one-body part of the Hamiltonian dominates the t_{fd} dependence of the internal energy, we report our results here as differences from the HF—either the PMHF solution or the broken-symmetry AFHF solution—in order to better expose the more interesting effects of correlations. This also makes sense given that the HF solutions must be upper bounds on the correct internal energy at $T = 0$. Moreover, we might expect the PMHF solution to be correct in the weak-coupling limit ($t_{fd} \to \infty$) and have observed previously that the AFHF energy is correct in the strong-coupling limit ($t_{fd} \to 0$) at low

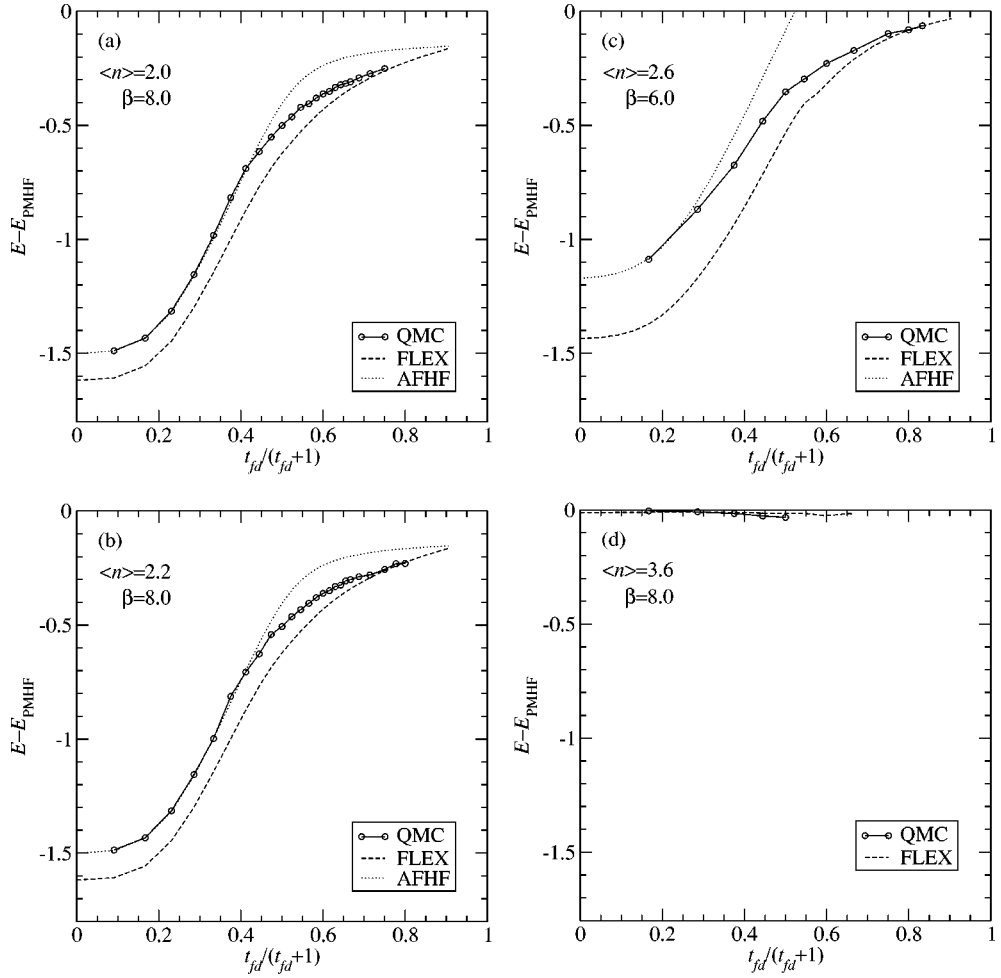

FIG. 6. The difference of the internal energy for various solutions from the PMHF solution, $E-E_{\mathrm{PMHF}}$, as a function of $t_{fd}/(t_{fd}+1)$, which is 0 and 1 at the strong- and weak-coupling limits, respectively. The results for QMC, FLEX, and AFHF are shown. (a) $\langle n\rangle=2.0$, (b) $\langle n\rangle=2.2$, (c) $\langle n\rangle=2.6$, (d) $\langle n\rangle=3.6$. In (d) $\varepsilon_f=-5.4$, and in (c) $\beta=6$. Other parameters are the same as in Fig. 2(a). In all cases QMC agrees with AFHF toward the strong-coupling limit and with FLEX toward the weak-coupling limit. In the rather extreme-filling case of (d), the energy difference $E-E_{\mathrm{PMHF}}$ is two orders of magnitude smaller than the other cases, implying that the correlations are negligible and the PMHF solution is quite accurate. In general, at the weak-coupling limit, PMHF gives the right solution except when the AFHF solution has a lower energy than the PMHF as in (a) and (b), which can happen for small finite systems; then, AFHF gives the right solution at the weak- as well as the strong-coupling limit.

temperature.[20,36] With these two limits in mind, we first present results as a function of the ratio $t_{fd}/(t_{fd}+1)$, where values 0 and 1 correspond to the strong- and weak-coupling limits, respectively.

Figure 6 presents our results for the correlation energy $E-E_{\mathrm{PMHF}}$ as a function of $t_{fd}/(t_{fd}+1)$ at four different fillings: $\langle n\rangle=2.0$ (a), 2.2 (b), 2.6 (c), and 3.6 (d). We calculate E with three different methods: QMC, diagrammatic FLEX, and mean-field AFHF. In the strong-coupling (atomic) limit, AFHF gives the correct energy at every filling, agreeing with QMC.[36] Toward the weak-coupling limit, FLEX agrees with QMC very well, giving not only the correct weak-coupling limit itself but also the correct leading-order dependence on $1/t_{fd}$. The PMHF solution is, in general, correct *at* the weak-coupling limit but, as is evident from Fig. 6(c), approaches this limit with an incorrect dependence on $1/t_{fd}$.

There is an apparent constant offset between the PMHF and other curves, including AFHF, at the weak-coupling limit in Figs. 6(a) and 6(b). Here one is at half filling or very close to it, and the AFHF solution on small lattices is lower in energy at the weak-coupling limit than the PMHF. In the thermodynamic limit, these offsets vanish, which is also suggested in the FLEX size dependence tests to be cited shortly.

In Fig. 6(d) there is no stable AFHF (or other magnetic) solution at any coupling strength. In addition $E-E_{\mathrm{PMHF}}$ is very small compared to Figs. 6(a)–6(c). Indeed correlations are not important in this case of extreme filling. Note that while the *total* fillings $\langle n\rangle$ vary in Figs. 6(a)–6(c), in each case $\langle n_f\rangle\sim 1$ and the correlation energies are of comparable size. In sharp contrast $\langle n_f\rangle\sim 1.8$ in Fig. 6(d), confirming the general understanding that correlations are largest near half filling of an interacting orbital and diminish for fillings of this orbital away from half filling.

The FLEX approximation is always paramagnetic if one does not include the anomalous-self-energy diagrams. Therefore, unlike the mean-field treatments of correlations, FLEX

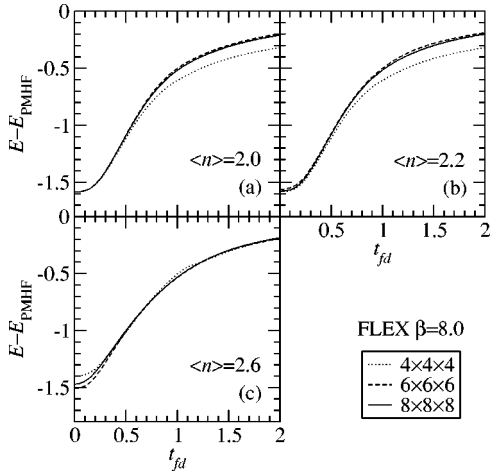

FIG. 7. The difference of the FLEX internal energy from the PMHF internal energy, plotted as a function of the hybridization t_{fd} for different lattice sizes for the purpose of evaluating the finite-size effects. (a) $\langle n\rangle = 2.0$, (b) $\langle n\rangle = 2.2$, (c) $\langle n\rangle = 2.6$. Parameters are the same as in Fig. 2. These finite-size effects are generally small.

has no anomalies arising from the solution switching from a broken symmetry (e.g., antiferromagnetic) to the uniform (paramagnetic) state as occurs in Fig. 6(c). Such HF transitions are absent in Figs. 6(a) and 6(b) since the AFHF solution is always stable.

The results in Fig. 6 were for $4\times4\times4$ periodic cells. To illustrate the effects of size dependence, Fig. 7 shows $E_{\mathrm{FLEX}}-E_{\mathrm{PMHF}}$ calculations done for $4\times4\times4$, $6\times6\times6$ and $8\times8\times8$ periodic cells. As expected the finite-size effects on the internal energy are generally small. This is because the internal energy is basically a local quantity. Note, however, the upward shift in $E_{\mathrm{FLEX}}-E_{\mathrm{PMHF}}$ with an increased cell size for larger t_{fd} in Figs. 7(a) and 7(b), which correspond to Figs. 6(a) and 6(b), respectively. These shifts are in the direction to remove the constant offsets at the weak-coupling limit between the PMHF and more rigorous methods in Figs. 6(a) and 6(b). It is also the case that the lowest $T=0$ HF solution at the weak-coupling limit is PMHF for all fillings in the thermodynamic limit.

G. Crossover behavior in the PAM

We now discuss some of the implications of these results for the potential presence of sharp switches in the PAM energy which could drive phase transitions in appropriate systems.

In the recent work[20] for the PAM at half filling $\langle n\rangle = 2.0$, we noted coincident anomalous behavior in three distinct low-temperature quantities as t_{fd} was increased beyond about 0.6: the singlet correlator increased abruptly; a Kondo resonance appeared and grew at the Fermi level; and the internal energy broke away from the AFHF result it had closely followed at smaller t_{fd}. We suggested that the abruptness of this change in internal energy, evidently associated with the screening of the local moments by the conduction electrons, was not inconsistent with the physics of the volume-collapse transitions in the rare-earth metals. Such

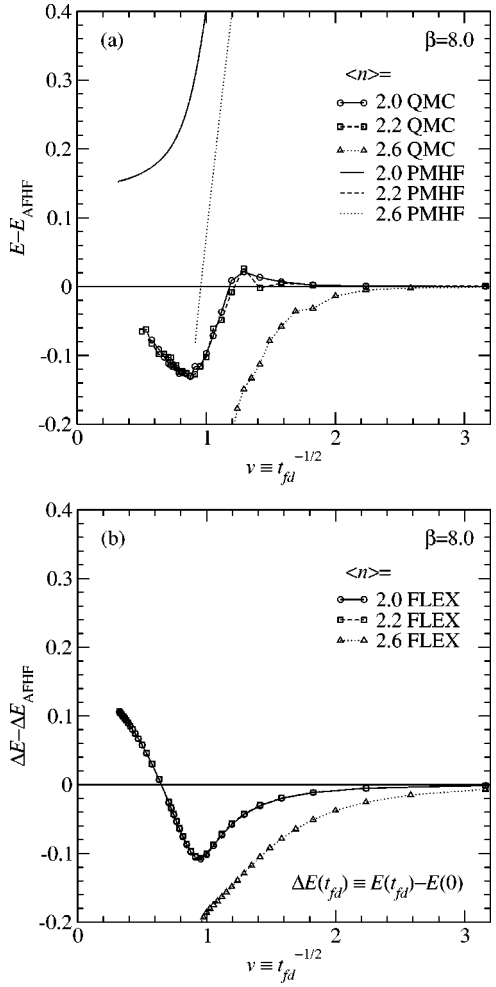

FIG. 8. (a) The dependence of the QMC and PMHF internal energies relative to the AFHF as a function of the inverse-square-root hybridization $v \equiv t_{fd}^{-1/2}$. Parameters are the same as in Fig. 2(a). For all three fillings, the QMC internal energy agrees with the AFHF internal energy at large v, breaking away at an intermediate v value. This breakaway, which happens at $v\sim1.3$ ($t_{fd}\sim0.6$) for $\langle n\rangle = 2.0$ and 2.2, and at $v\sim2.2$ ($t_{fd}\sim0.2$) for $\langle n\rangle = 2.6$, might have implications on the volume-collapse phenomenon. (b) The FLEX results for the same parameters, with the atomic-limit ($t_{fd}=0$) offsets removed. The agreement with QMC is quite reasonable although the breakaway is more gradual than seen for the QMC results in (a).

a possibility also was previously discussed in the context of the Anderson impurity model.[16] We now revisit this issue from a different perspective than given in our earlier work.[20]

Figure 8(a) shows our QMC and PMHF internal energies relative to the AFHF results, $E-E_{\mathrm{AFHF}}$, for all three fillings at the low temperature of $T=0.125$. Since the physical dependence of the hybridization on volume is $t_{fd}\sim V^{-2}$, we have chosen $v\equiv t_{fd}^{-1/2}\propto V$ to label our horizontal axis. Note first the AFHF to PMHF transition at $v=0.96$ ($t_{fd}=1.09$) which occurs as v is decreased for the filling $\langle n\rangle = 2.6$. While there are no HF transitions at the two other fillings for the $4\times4\times4$ cell, such transitions do occur in the thermodynamic limit at $v=0.87$ and 0.74 ($t_{fd}=1.33$ and 1.83) for $\langle n\rangle = 2.6$ and 2.2, respectively, but there is none exactly at

$\langle n\rangle = 2.0$. These mean-field calculations describe a transition from a ''localized'' AFHF phase, with the *f* bands Hubbard split away from the Fermi level, to an ''itinerant'' PMHF phase, with the merged *f* bands overlapping the Fermi level, in fundamentally the same way as realistic HF and modified local-density methods describe the volume-collapse transitions in the rare-earth metals.[18] While having some degree of validity, it has been argued in Ref. 18 that the realistic HF and modified local-density-approximation transitions occur too close to the itinerant limit for the rare earths, corresponding to too-small values of v in the present PAM analog. The QMC results in Fig. 8(a) appear to support this suggestion.[37] While both AFHF and PMHF values must be upper bounds on the exact QMC at $T=0$, it is interesting that at large v the QMC values are quite close to the AFHF upper bound, whereas at smaller v they appear to bend and stay well away from the downward-moving PMHF bounds. The net effect is a downturn in the QMC energies with decreasing v well before the PMHF curves cross below the AFHF, as evident for $\langle n\rangle = 2.6$ and likely to be so in the thermodynamic limit for $\langle n\rangle = 2.2$. This is at least suggestive of the correlated version of the collapse transition, although, a compelling case is hindered by the internal-energy contributions omitted by the PAM.

It should also be emphasized that as v is decreased, the onset of the downturns in the QMC energies in Fig. 8(a), $v \sim 1.3$, 1.3, and 2.2 ($t_{fd} \sim 0.6$, 0.6, and 0.2) for $\langle n\rangle = 2.0$, 2.2, and 2.6, respectively, coincides with the onset of rapid increases in magnitude of the singlet correlator and with similar rapid decreases in the low-temperature entropy as discussed earlier. Moreover, from the $\langle n\rangle = 2.6$ case, we know that all these features occur and coincide in the absence of antiferromagnetic correlations, so that their fundamental origin is likely associated solely with the screening of the local moments by the conduction electrons.

As noted earlier the FLEX approximation does not produce the Mott gap and therefore may overestimate Kondo-like excitations for smaller t_{fd}, which never disappear from the spectrum, even at the atomic (strong-coupling) limit. This failure of FLEX leads to an underestimation of the internal energy as seen at $t_{fd}=0$ in Fig. 6, due to the spurious presence of Kondo-like excitations at this limit. Nevertheless, it is interesting to focus only on the t_{fd} dependence and remove these atomic-limit offsets by using $\Delta E(t_{fd}) \equiv E(t_{fd}) - E(0)$ and plotting $\Delta E - \Delta E_{\mathrm{AFHF}}$ in the case of FLEX, as is done in Fig. 8(b). As may be seen, the agreement with Fig. 8(a) is really quite good, although, the breakaway from the AFHF is more gradual than in the QMC. It is tempting to attribute this more gradual behavior in Fig. 8(b) to the persistence of Kondo-like excitations in FLEX to the largest $v \equiv t_{fd}^{-1/2}$, whereas presumably such excitations cease for the QMC results in Fig. 8(a) beyond some critical values of v, possibly where the QMC and AFHF curves become essentially degenerate.

IV. SUMMARY AND CONCLUSIONS

In this paper we have extended our previous studies[20] of the periodic Anderson model (PAM) to nonsymmetric cases, examining the low-temperature dependence of a variety of quantities as a function of the hybridization t_{fd} between the *f* and *d* orbitals: local moment, singlet correlator, antiferromagnetic structure factor, entropy, and internal energy. Results from the determinant quantum Monte Carlo (QMC), fluctuation-exchange approximation (FLEX), and Hartree-Fock (HF) methods have been compared.

Beyond exploration of the properties of the nonsymmetric PAM itself, these results provide further insight into the effect of more exact treatments of correlations on mean-field approximations to phase transitions driven by changes to the ratio of atomic hybridization to Coulomb repulsion, such as the volume-collapse transitions in the rare-earth metals. Indeed this problem has also motivated many of our parameter choices for the PAM, which were generally selected to maintain approximately one *f* electron per site while varying the number of *d* electrons and consequently the total filling $\langle n\rangle$.

One of the fundamental results of this work is the coincidence of systematic changes in the measured quantities across particular values of the hybridization, $t_{fd} \sim 0.6$, 0.6, and 0.2 for $\langle n\rangle = 2.0$, 2.2, and 2.6, respectively. For t_{fd} less than these values, the local moment (~ 1), singlet correlator (~ 0), and *f*-subsystem entropy ($\sim \ln 2$) are all approximately constant, while the internal energy is well approximated by AFHF, i.e., a regime of well-formed, unscreened local moments. For t_{fd} greater than these values, the local moment and entropy drop, the magnitude of the singlet correlator grows, and the internal energy falls below that of AFHF. The singlet correlator suggests Kondo-like effects in this regime, although, there is a complete absence of antiferromagnetic correlations only at the largest filling, $\langle n\rangle = 2.6$, where this identification appears unambiguous. It should be acknowledged that changes with t_{fd} for $\langle n\rangle = 2.6$ are also somewhat more gradual than those closer to half filling, and for this reason we used slightly different criteria for the crossover t_{fd} values: the first significant breakaway from the constant values for $\langle n\rangle = 2.6$ vs a location of particularly rapid change for $\langle n\rangle = 2.0$ and 2.2.

We have presented the correlation energy $E - E_{\mathrm{PMHF}}$ most of the way between the strong- and weak-coupling limits by varying t_{fd} from 0 to very large values. The exact QMC energies interpolate smoothly between the AFHF result at the strong and PMHF result at the weak-coupling limit for $\langle n\rangle = 2.6$, and we expect similar behavior at other fillings in the thermodynamic limit. Approximate diagrammatic FLEX agrees very well with QMC towards weak coupling and is distinctly improved over PMHF by not only reaching the correct weak-coupling limit but also including the leading order dependence on t_{fd}^{-1} away from this limit. Moreover, the FLEX curve is smooth like QMC and generally of the same shape throughout the full t_{fd} range, although, it increasingly underestimates the internal energy as the strong-coupling limit is approached since the FLEX approximation does not produce the Mott gap. Even so this is a gradual effect and the t_{fd} dependence compares favorably to QMC even within the strong- and intermediate-coupling regimes, $0 \leqslant t_{fd} \leqslant 2$. In general the FLEX results are in remarkably good overall agreement with QMC, suggesting this approach as a useful approximation for the study of *f*-electron systems.

Due to the crudeness of the PAM model, it is difficult to make a compelling argument on thermodynamic grounds that it exhibits some transition similar to the volume-collapse transition in the rare-earth metals. However, mean-field HF calculations for the PAM and for realistic all-valence-orbital treatments of the rare earth metals both yield transitions of the same fundamental nature, and the latter are certainly caricatures of the volume-collapse transitions. It thus makes sense to ask how the correlated and HF results differ for the PAM and to presume similar differences should be obtained in the realistic case. We find that for decreasing $t_{fd}^{-1/2}$ (or, volume) the correlated energies break away from the ''localized'' AFHF results at values of $t_{fd}^{-1/2}$ (or, volume) considerably larger than where the ''itinerant'' PMHF energies cross down through the AFHF curve and become stable. Moreover, this breakaway coincides with the decrease in the local moment and *f*-subsystem entropy, and the increase in the singlet correlator. The coupling of the thermodynamics with the singlet correlator behavior is certainly consistent with the Kondo volume-collapse scenario,[16] while it is interesting that the associated decay in the local moment is reminiscent of the Mott-transition perspective.[17]

ACKNOWLEDGMENTS

We would like to thank Wei Ku for useful discussions and a critical reading of the manuscript. Work at University of California, Davis, was supported in part by Accelerated Strategic Computing Initiative Grants, IUT Agreement Nos. B507147 and B511275 with Lawrence Livermore National Laboratory (LLNL), and by NSF-DMR-0312261 and NSF-INT-0203837. T.P. would also like to acknowledge CNPq Brazil for financial support. Work at LLNL was performed under the auspices of the U.S. Department of Energy by the University of California, Lawrence Livermore National Laboratory, under Contract No. W-7405-ENG-48. We also thank the staff at the Materials Research Institute at LLNL for their support.

*Email address: tclp@if.ufrj.br

†Email address: esirgen@usc.edu

[1] G.R. Stewart, Rev. Mod. Phys. **56**, 755 (1984); P.A. Lee, T.M. Rice, J.W. Serene, L.J. Sham, and J.W. Wilkins, Comments Condens. Matter Phys. **12**, 99 (1986); A. C. Hewson, *The Kondo Problem to Heavy Fermions* (Cambridge University Press, Cambridge, 1993).

[2] S. Doniach, Physica B & C **91**, 231 (1977).

[3] M.A. Ruderman and C. Kittel, Phys. Rev. **96**, 99 (1954).

[4] C. D. Batista, J. Bonča, and J. E. Gubernatis, Phys. Rev. B **68**, 064403 (2003).

[5] P. Nozières, Ann. Phys. (Paris) **10**, 19 (1985).

[6] A.N. Tahvildar-Zadeh, M. Jarrell, T. Pruschke, and J.K. Freericks, Phys. Rev. B **60**, 10 782 (1999); .N.S. Vidhyadhiraja, A.N. Tahvildar-Zadeh, M. Jarrell, and H.R. Krishnamurthy, Europhys. Lett. **49**, 459 (2000).

[7] V. Barzykin and I. Affleck, Phys. Rev. B **57**, 432 (1998).

[8] I. Affleck and P. Simon, Phys. Rev. Lett. **86**, 2854 (2001).

[9] J. Gan, J. Phys.: Condens. Matter **6**, 4547 (1994).

[10] J.P. Boyce and C.P. Slichter, Phys. Rev. Lett. **32**, 61 (1974); Phys. Rev. B **13**, 379 (1996).

[11] K. Held, C. Huscroft, R.T. Scalettar, and A.K. McMahan, Phys. Rev. Lett. **85**, 373 (2000).

[12] Two-dimensional quantum Monte Carlo studies of the PAM include: Y. Zhang, and J. Callaway, Phys. Rev. B **38**, 641 (1988); M. Vekic, J.W. Cannon, D.J. Scalapino, R.T. Scalettar, and R.L. Sugar, Phys. Rev. Lett. **74**, 2367 (1995). In three dimensions, see Ref. 20.

[13] A two-dimensional QMC study of the PAM using the ''constrained-path'' method to reach low temperatures is contained in J. Bonča and J.E. Gubernatis, Phys. Rev. B **58**, 6992 (1998).

[14] Dynamical mean-field-theory studies of the PAM include: M. Jarrell, Phys. Rev. B **51**, 7429 (1995); A.N. Tahvildar-Zadeh, M. Jarrell, and J.K. Freericks, *ibid.* **55**, 3332 (1997); M. Rozenberg, *ibid.* **52**, 7369 (1995); T. Schork and S. Blawid, *ibid.* **56**, 6559 (1997); T. Pruschke, R. Bulla, and M. Jarrell, *ibid.* **61**, 12 799 (2000); D. Meyer and W. Nolting, *ibid.* **62**, 5657 (2000); **61**, 13 465 (2000); Y. Shimizu, O. Sakai, and A.C. Hewson, J. Phys. Soc. Jpn. **69**, 1777 (2000); K. Held and R. Bulla, Eur. Phys. J. B **17**, 7 (2000).

[15] The physical motivation for the choice of on-site hybridization is open to question since one can always choose an orbital basis in which the one-particle Hamiltonian is diagonal at a given lattice site.

[16] J.W. Allen and R.M. Martin, Phys. Rev. Lett. **49**, 1106 (1982); J.W. Allen and L.Z. Liu, Phys. Rev. B **46**, 5047 (1992); M. Lavagna, C. Lacroix, and M. Cyrot, Phys. Lett. **90A**, 210 (1982); J. Phys. F: Met. Phys. **13**, 1007 (1983).

[17] B. Johansson, Philos. Mag. **30**, 469 (1974); B. Johansson and A. Rosengren, Phys. Rev. B **11**, 2836 (1975); B. Johansson, I.A. Abrikosov, M. Aldén, A.V. Ruban, and H.L. Skriver, Phys. Rev. Lett. **74**, 2335 (1995).

[18] A. McMahan, C. Huscroft, R.T. Scalettar, and E.L. Pollock, J. Comput.-Aided Mater. Des. **5**, 131 (1998).

[19] A.K. McMahan, K. Held, and R.T. Scalettar, Phys. Rev. B **67**, 075108 (2003).

[20] C. Huscroft, A.K. McMahan, and R.T. Scalettar, Phys. Rev. Lett. **82**, 2342 (1999).

[21] J.E. Hirsch and S. Tang, Phys. Rev. Lett. **62**, 591 (1989).

[22] S.R. White, D.J. Scalapino, R.L. Sugar, E.Y. Loh, J.E. Gubernatis, and R.T. Scalettar, Phys. Rev. B **40**, 506 (1989).

[23] This decreased sensitivity of long-range AF order to doping is almost certainly tied to the fact that in the two-band model we keep $\langle n_f \rangle = 1$ and are doping the conduction band.

[24] Our extensive studies in recent years indicate that the FLEX approximation does not produce the Mott-Hubbard gap in general (except for certain parameters). But there is usually a hump structure reminiscent of the Hubbard bands, which are caused by the strong spin fluctuations, surrounding the central Kondo-like resonance. The more complicated diagrammatic parquet approximation also fails to generate the Mott-Hubbard gap [N. E. Bickers (unpublished)].

[25] For treatments that incorporate first-principles band structures and interaction strengths, see M.B. Zölfl, I.A. Nekrasov, Th. Pruschke, V.I. Anisimov, and J. Keller, Phys. Rev. Lett. **87**,

276403 (2001); and K. Held, A. McMahan, and R.T. Scalettar, *ibid.* **87**, 276404 (2001).

[26] R. Blankenbecler, R.L. Sugar, and D.J. Scalapino, Phys. Rev. D **24**, 2278 (1981).

[27] E.Y. Loh, J.E. Gubernatis, R.T. Scalettar, S.R. White, D.J. Scalapino, and R.L. Sugar, Phys. Rev. B **41**, 9301 (1990).

[28] N.E. Bickers and D.J. Scalapino, Ann. Phys. (N.Y.) **193**, 206 (1989).

[29] G. Baym and L.P. Kadanoff, Phys. Rev. **124**, 287 (1961); G. Baym, *ibid.* **127**, 1391 (1962).

[30] C. de Dominicis and P.C. Martin, J. Math. Phys. **5**, 14 (1964).

[31] C.-H. Pao and N.E. Bickers, Phys. Rev. Lett. **72**, 1870 (1994); P. Monthoux and D.J. Scalapino, *ibid.* **72**, 1874 (1994).

[32] N.E. Bickers, D.J. Scalapino, and S.R. White, Phys. Rev. Lett. **62**, 961 (1989); N.E. Bickers and S.R. White, Phys. Rev. B **43**, 8044 (1991); G. Esirgen and N.E. Bickers, *ibid.* **55**, 2122 (1997); **57**, 5376 (1998); G. Esirgen, H.-B. Schüttler, and N.E. Bickers, Phys. Rev. Lett. **82**, 1217 (1999); G. Esirgen, H.-B. Schüttler, C. Gröber, and H.G. Evertz, Phys. Rev. B **64**, 195105 (2001).

[33] C.-H. Pao and N.E. Bickers, Phys. Rev. B **49**, 1586 (1994).

[34] The magnetic susceptibilities plotted are the FLEX susceptibilities (bubble-diagram sums) which go directly into the FLEX self-energy. They are *not* the conserving FLEX susceptibilities calculated by the functional differentiation of the generating functional. The extra diagrams that enter the conserving susceptibilities tend to increase the magnitude of the magnetic susceptibilities, but qualitative behavior of the magnetic susceptibilities remains the same.

[35] T. Paiva, R.T. Scalettar, C. Huscroft, and A.K. McMahan, Phys. Rev. B **63**, 125116 (2001).

[36] It is to be emphasized that the AFHF and QMC internal energies agree in the strong-coupling (small-t_{fd}) limit only at low temperatures. The temperature dependence is qualitatively similar to Fig. 6(c) with the x axis being the temperature, where the AFHF energy switches to the PMHF at higher temperature and the QMC interpolates smoothly between the low-and high-temperature limits.

[37] The data shown in Fig. 8(a) differ slightly from Ref. 20. in that the energy difference has a small upturn before becoming negative with decreasing volume. This is because the present data now include a correction for the errors associated with the finite discretization of inverse temperature.